Reciprocal cross-regulation of VND and SND multigene TF families for wood formation in *Populus trichocarpa*

Ying-Chung Jimmy Lin[a,b,c,d,1], Hao Chen[d,1], Quanzi Li[e,1], Wei Li[a,d], Jack P. Wang[a,d], Rui Shi[f], Sermsawat Tunlaya-Anukit[d], Peng Shuai[d,g], Zhifeng Wang[a], Hongyan Ma[a], Huiyu Li[a,d], Ying-Hsuan Sun[h], Ronald R. Sederoff[d,2], and Vincent L. Chiang[a,d,2]

[a]State Key Laboratory of Tree Genetics and Breeding, Northeast Forestry University, Harbin, 150040 China; [b]Department of Life Sciences, College of Life Science, National Taiwan University, Taipei 10617, Taiwan; [c]Institute of Plant Biology, College of Life Science, National Taiwan University, Taipei 10617, Taiwan; [d]Forest Biotechnology Group, Department of Forestry and Environmental Resources, North Carolina State University, Raleigh, NC 27695; [e]State Key Laboratory of Tree Genetics and Breeding, Research Institute of Forestry, Chinese Academy of Forestry, Beijing 100091, China; [f]Crop and Soil Sciences Department, North Carolina State University, Raleigh, NC 27695; [g]College of Forestry, Fujian Agriculture and Forestry University, Fuzhou 350002, China; and [h]Department of Forestry, National Chung Hsing University, Taichung 40227, Taiwan

Contributed by Ronald R. Sederoff, September 27, 2017 (sent for review August 15, 2017; reviewed by Kyung-Hwan Han and Misato Ohtani)

Secondary cell wall (SCW) biosynthesis is the biological process that generates wood, an important renewable feedstock for materials and energy. NAC domain transcription factors, particularly Vascular-Related NAC-Domain (VND) and Secondary Wall-Associated NAC Domain (SND) proteins, are known to regulate SCW differentiation. The regulation of VND and SND is important to maintain homeostasis for plants to avoid abnormal growth and development. We previously identified a splice variant, *PtrSND1-A2^{IR}*, derived from *PtrSND1-A2* as a dominant-negative regulator, which suppresses the transactivation of all *PtrSND1* family members. PtrSND1-A2^{IR} also suppresses the self-activation of the PtrSND1 family members except for its cognate transcription factor, PtrSND1-A2, suggesting the existence of an unknown factor needed to regulate *PtrSND1-A2*. Here, a splice variant, *PtrVND6-C1^{IR}*, derived from *PtrVND6-C1* was discovered that suppresses the protein functions of all *PtrVND6* family members. PtrVND6-C1^{IR} also suppresses the expression of all *PtrSND1* members, including *PtrSND1-A2*, demonstrating that PtrVND6-C1^{IR} is the previously unidentified regulator of *PtrSND1-A2*. We also found that PtrVND6-C1^{IR} cannot suppress the expression of its cognate transcription factor, *PtrVND6-C1*. *PtrVND6-C1* is suppressed by PtrSND1-A2^{IR}. Both PtrVND6-C1^{IR} and PtrSND1-A2^{IR} cannot suppress their cognate transcription factors but can suppress all members of the other family. The results indicate that the splice variants from the *PtrVND6* and *PtrSND1* family may exert reciprocal cross-regulation for complete transcriptional regulation of these two families in wood formation. This reciprocal cross-regulation between families suggests a general mechanism among NAC domain proteins and likely other transcription factors, where intron-retained splice variants provide an additional level of regulation.

reciprocal cross-regulation | NAC transcription factors | alternative splicing | wood formation | *Populus trichocarpa*

Wood is an abundant and renewable raw material for energy, pulping, and solid wood products (1, 2). Wood is composed of secondary cell walls (SCWs), which in turn are made of three major polymers: cellulose, hemicelluloses, and lignin. SCW biosynthesis is a complex developmental process, which is regulated by control of transcription (3–5), mRNA splicing (6, 7), protein modification (8), and metabolic flux (9). Few studies of the transcriptional regulation of wood formation have been carried out in woody plants, although SCW biosynthesis has been studied extensively in *Arabidopsis* (3–5, 10–16). *NAC* (for NAM, ATAF1/2, and CUC2) and *MYB* transcription factors (TFs) regulate SCW differentiation (3–5). NAC domain proteins, in particular the VND6 and SND1 families, have been proposed as "master regulators" of SCW biosynthesis in *Arabidopsis* (10, 11). VND6 and SND1 activate downstream TFs, such as *MYB*s, to induce indirect expression of genes for cellulose, hemicelluloses, and lignin biosynthesis (3, 14, 17). In *Arabidopsis*, VND6 induces the differentiation of metaxylem and protoxylem vessel elements (3, 10, 12), while SND1 regulates deposition of SCWs in fibers (11, 12). Overexpression of *VND6* or *SND1* causes abnormal xylem or stunted growth (5, 10, 11). The regulation of these TFs is important for normal plant growth and development.

In *Populus trichocarpa*, the *VND6* family has six members (*PtrVND6-A1*, *-A2*, *-B1*, *-B2*, *-C1*, *-C2*), and the *SND1* family has four members (*PtrSND1-A1*, *-A2*, *-B1*, *-B2*) (6). We previously identified a high-level regulator, *PtrSND1-A2^{IR}*, of the *SND1* family (6). *PtrSND1-A2^{IR}* is an intron-retained (IR) splice variant of *PtrSND1-A2* that acts as a dominant negative to suppress the protein functions of *PtrSND1* family members (6). PtrSND1-A2^{IR} lacks the DNA binding and transcriptional activation domains but retains the protein dimerization domain. PtrSND1-A2^{IR} is found exclusively in cytoplasmic foci. Through the formation of heterodimers with any of the PtrSND1 members, PtrSND1-A2^{IR} can be translocated into the nucleus, where it suppresses the protein functions of the PtrSND1 family members (6). PtrSND1-A2^{IR} also suppresses the self-activation of the *PtrSND1* family members except for *PtrSND1-A2*, its cognate TF (6). How the expression of *PtrSND1-A2* itself is regulated has remained unknown.

Significance

Wood is a widely used renewable feedstock for industrial production and energy generation. The secondary cell wall (SCW) is the major component of wood. Two key transcription factor families, Vascular-Related NAC-Domain (VND) and Secondary Wall-Associated NAC Domain (SND), are master gene regulators for SCW biosynthesis. However, plants exhibit stunted growth or abnormal SCW development under excess VND or SND gene expression. In this study, we show that two splice variants, PtrVND6-C1^{IR} and PtrSND1-A2^{IR}, each from VND and SND families, act as negative regulators. We propose that PtrVND6-C1^{IR} and PtrSND1-A2^{IR} function together for reciprocal cross-regulation of VND and SND families to maintain homeostasis for xylem differentiation and plant development.

Author contributions: Y.-C.J.L., H.C., Q.L., W.L., R.R.S., and V.L.C. designed research; Y.-C.J.L. performed research for Figs. 2, 4, and 5; H.C. performed research for all figures except Fig. 1*B* and Fig. 4; R.S. performed research for Dataset S1; S.T.-A. performed research for Fig. 1*B*; Y.-C.J.L., H.C., J.P.W., P.S., Z.W., H.M., H.L., Y.-H.S., and V.L.C. analyzed data; and Y.-C.J.L., H.C., J.P.W., R.R.S., and V.L.C. wrote the paper.

Reviewers: K.-H.H., Michigan State University; and M.O., Nara Institute of Science and Technology.

The authors declare no conflict of interest.

[1]Y.-C.J.L., H.C., and Q.L. contributed equally to this work.

[2]To whom correspondence may be addressed. Email: ron_sederoff@ncsu.edu or vchiang@ncsu.edu.

This article contains supporting information online at www.pnas.org/lookup/suppl/doi:10.1073/pnas.1714422114/-/DCSupplemental.

Many dominant negatives are derived from alternative splicing (18, 19). They usually lack DNA binding or transactivation domains but retain protein–protein interaction domains (20). In animals, dominant negatives derived from alternative splicing form heterodimers with their targets to disrupt the function of the target proteins (21, 22). In plants, this dominant-negative effect was first reported in *Arabidopsis*, where alternative splicing variants suppressed the protein function of their cognate TFs (23, 24). The dominant-negative effect suppressing members of a TF family was first reported in *P. trichocarpa* (6). There is no previous report on the regulation of one dominant negative on multiple TF families.

In this article, we report the discovery of an IR splice variant, *PtrVND6-C1^{IR}*, derived from *PtrVND6-C1* in the *PtrVND6* family, which also acts as a dominant negative on its own family and on the *PtrSND1* family. We performed laser capture microdissection (LCM) combined with RNA-sequencing (RNA-seq) and determined that all *PtrVND6* and *PtrSND1* family members, *PtrSND1-A2^{IR}*, and *PtrVND6-C1^{IR}* were expressed in the same cell types. A transactivation assay in stem-differentiating xylem (SDX) protoplasts was used to characterize their functions on transcriptional regulation. Combining these results with subcellular localization and bimolecular fluorescence complementation (BiFC), we have uncovered a reciprocal cross-regulation system of *PtrVND6* and *PtrSND1* families by their IR splice variants, *PtrSND1-A2^{IR}* and *PtrVND6-C1^{IR}*, in SCW biosynthesis.

Results

Identification of Six Xylem-Specific PtrVND6s. There are two VND families, VND6 and VND7, in the *P. trichocarpa* genome (6). We first identified which members of these VND families are preferentially expressed in the wood-forming tissue (SDX). To do this, we prepared total RNA from SDX (X), phloem (P), young shoots (S), and leaves (L) and carried out full transcriptome RNA-seq analysis. Two hundred and nine SDX differentially expressed TFs (FDR < 0.05) were identified by comparison of X/P, X/S, and X/L tissue pairs with all three transcript abundance ratios >1.5 (Fig. S1 and Dataset S1). These 209 TFs belong to 41 diverse TF families, including 21 in the NAC family. These 21 are as follows: four *PtrSND1*s, six *PtrVND6*s, six *PtrSND2/3*s (6), and five *PNAC*s (Dataset S1). The six *PtrVND6*s are *PtrVND6-A1* (POPTR_0015s14770, Potri.015G127400), *PtrVND6-A2* (POPTR_0012s14660, Potri.012G126500), *PtrVND6-B1* (POPTR_0003s11250, Potri.003G113000), *PtrVND6-B2* (POPTR_0001s00220, Potri.001G120000), *PtrVND6-C1* (POPTR_0007s13910, Potri.007G014400), and *PtrVND6-C2* (POPTR_0005s11870, Potri.005G116800) (6). We then cloned the cDNAs of all six *PtrVND6*s.

Three Splice Variants of *PtrVND6*s Were Identified Through PCR Cloning and RNA-Seq. Each gene sequence of the *PtrVND6*s contains three exons and two introns (*P. trichocarpa* version *JGI* 2.2), indicating that all *PtrVND6* cDNAs should be about 1.1 kb (Fig. S2 *A–D*). We PCR cloned all six *PtrVND6* cDNAs, and all have the expected size and correct sequence (Fig. 1*A*). In addition to the expected PCR products of six *PtrVND6*s (~1.1 kb), three larger fragments were detected for *PtrVND6-A1* (~1.3 kb), *-A2* (~1.3 kb), and *-C1* (~1.8 kb) (Fig. 1*A*). These fragments represent cDNAs that retain intron 2 (I2) of *PtrVND6-A1* (Fig. S2*E*), *PtrVND6-A2* (Fig. S2*F*), and *PtrVND6-C1* (Fig. S2*G*). The retained introns are due to incomplete mRNA splicing. The inclusion of the retained introns was confirmed by sequence reads with the specific retained introns based on 18 independent RNA-seq analyses (Fig. 1*B* for *PtrVND6-C1* and Fig. S3 for *PtrVND6-A1*, *-A2*, and *-C1*). We named these IR splice variants as *PtrVND6-A1^{IR}*, *-A2^{IR}*, and *-C1^{IR}*. These three variants are also preferentially expressed in SDX compared with phloem, young shoots, and leaves (Fig. 1*C* for *PtrVND6-C1^{IR}* and Fig. S4 for *PtrVND6-A1^{IR}*, *-A2^{IR}*, and *-C1^{IR}*).

We next investigated whether the mRNAs of the three splice variants are translated into proteins.

***PtrVND6-C1^{IR}* Encodes an Incomplete NAC Domain Protein in *P. trichocarpa* SDX.** The inferred protein structures of PtrVND6-A1, -A2, and -C1 include an N-terminal NAC domain with β′, α1a/b, and β1–β6 subdomains and a C-terminal activation domain (Fig. 1 *D*, *ii* and *iv* for PtrVND6-C1 and Fig. S2 *B–D* for PtrVND6-A1, -A2, and -C1). A premature termination codon (PTC) in the retained introns of *PtrVND6-A1^{IR}*, *-A2^{IR}*, and *-C1^{IR}* yields smaller proteins, which lack a C-terminal activation domain (Fig. 1 *D*, *iii* and *v* for PtrVND6-C1^{IR} and Fig. S2 *E–G* for PtrVND6-A1^{IR}, -A2^{IR}, and -C1^{IR}). Of these three variants, we focused on *PtrVND6-A1^{IR}* and *PtrVND6-C1^{IR}* (Fig. S3), both of which have the highest expression. We designed immunogens using polypeptides specific to the NAC domains of PtrVND6-A1 and -A1^{IR} and the NAC domains of PtrVND6-C1 and -C1^{IR} to produce their corresponding polyclonal antibodies. The antibodies were tested for specificity using recombinant proteins of the six full-size PtrVND6s and the variants PtrVND6-A1^{IR}, -A2^{IR}, and -C1^{IR} produced by *Escherichia coli* (Fig. S5*A* for PtrVND6-A1 and -A1^{IR} and Fig. S5*B* for PtrVND6-C1 and -C1^{IR}). The antibodies were then used for Western blot analysis of nuclear proteins isolated from SDX. PtrVND6-A1 reacted with the antibody, showing a size of 42.3 kDa as predicted (Fig. S5*D*). No signal was detected for PtrVND6-A1^{IR} (Fig. S5*D*), indicating that either the mRNA of *PtrVND6-A1^{IR}* is not translated or its protein quantity is too low to detect. Strong signals were detected for PtrVND6-C1 and PtrVND6-C1^{IR} around the predicted masses of 39.8 and 21.1 kDa, respectively (Fig. 1 *E*, *i* and Fig. S5*E*).

To further confirm the presence of the PtrVND6-C1^{IR} protein, we designed a polypeptide specific to its 28 unique amino acids upstream of the PTC (gray box in Fig. 1 *D*, *v*) and produced a polyclonal antibody. Antibody specificity was verified (Fig. S5*E*), and this antibody was able to discriminate PtrVND6-C1^{IR} from PtrVND6-C1 and other PtrVND6s (Fig. S5*C*). Western blot analysis of the SDX nuclear protein shows a band around 21 kDa, confirming the presence and size of PtrVND6-C1^{IR} (Fig. 1 *E*, *ii* and Fig. S5*F*). PtrVND6-C1^{IR} is the only detected variant of PtrVND6; thus, we investigated the role of PtrVND6-C1^{IR} in wood formation and its potential regulatory relationship with other full-size PtrVND6s.

PtrVND6-C1^{IR} Inhibits the Transcription of *PtrMYB021*. In *Arabidopsis*, AtVND6 can directly induce the expression of *AtMYB46* (17). We used our *P. trichocarpa* SDX protoplast system (6, 25) to test for transregulation activity of PtrVND6-C1^{IR} and the six full-size PtrVND6s. All six full-size PtrVND6s increased the expression of *PtrMYB021* by 1.43–4.19-fold (Fig. 1*F*). PtrVND6-C1^{IR} reduced *PtrMYB021* gene expression by 54% ($P < 0.02$) (Fig. 1*F*). The inferred protein structure of PtrVND6-C1^{IR} has a complete DNA binding domain (except for the β6 motif; Fig. 1 *D*, *v*) and has no activation domain (Fig. 1 *D*, *v*). This result suggests that PtrVND6-C1^{IR} can compete with the direct binding of the six full-size PtrVND6s to the *PtrMYB021* promoter and decrease the expression of *PtrMYB021*.

We then used an electrophoretic mobility shift assay (EMSA) (6) to test for the direct binding of full-size PtrVND6s and PtrVND6-C1^{IR} to the *PtrMYB021* promoter. Retardation of DNA probe mobility and probe competition showed that each of the six full-size PtrVND6s can bind to the *PtrMYB021* promoter (PtrVND6-C1 and -C1^{IR} in Fig. 1*G* and all PtrVND6s in Fig. S6). Contrary to expectation, PtrVND6-C1^{IR} did not bind to the *PtrMYB021* promoter (Fig. 1*G*). This result indicates that the absence of the β6 motif of PtrVND6-C1^{IR} disrupts its DNA binding ability. The transactivation and EMSA assays show that *PtrMYB021* is a common and direct target of all six full-size PtrVND6s and suggest that PtrVND6-C1^{IR} represses the

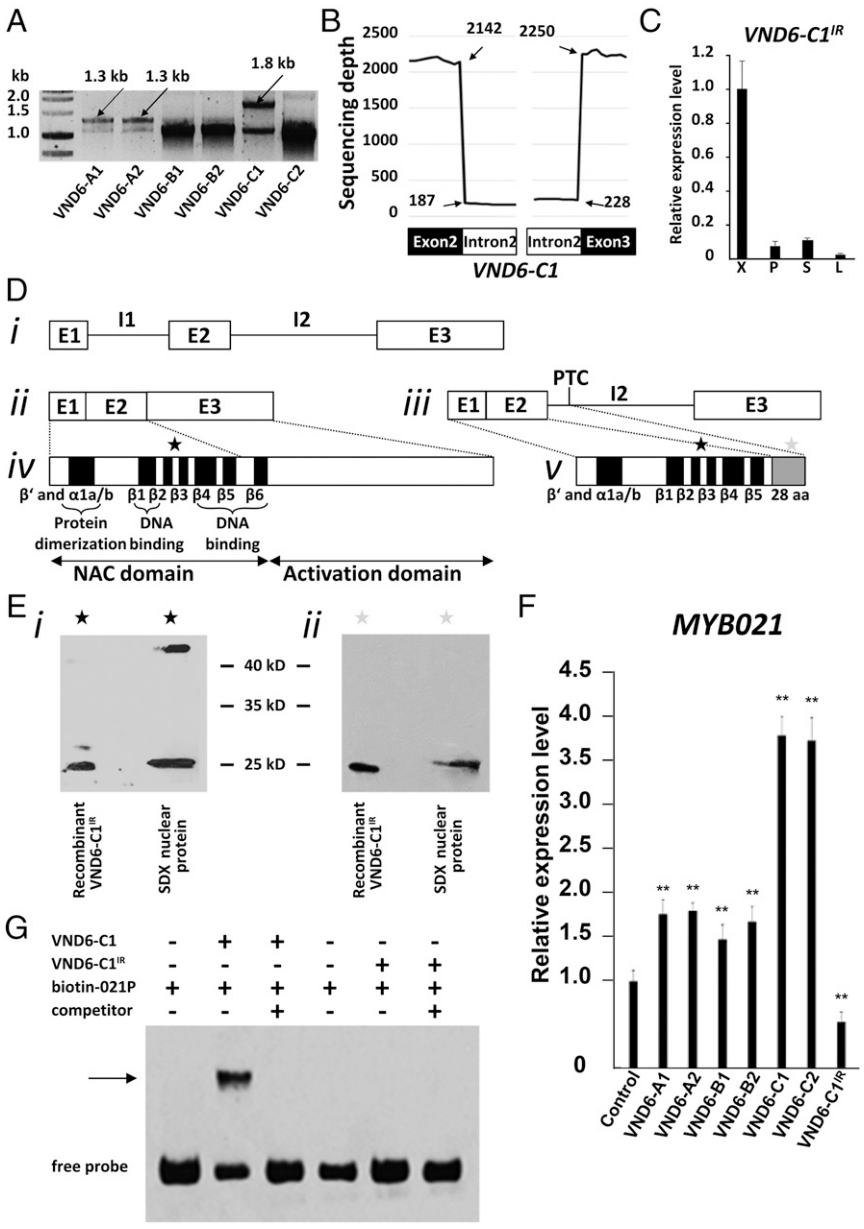

Fig. 1. Discovery of PtrVND6-C1^{IR} and its functional analysis. (*A*) RT-PCR of six of the PtrVND6 family members. (*B*) Sequencing depth of 40 nt on the junctions of *PtrVND6-C1* exon 2 (20 nt in the left black box) and I2 (20 nt in the left white box), and I2 (20 nt in the right white box) and exon 3 (20 nt in the right black box). We manually aligned the 5′ and 3′ junctions of each PtrVND6 gene and found no specific sequence for IR genes. (*C*) qRT-PCR analysis of the transcript abundance of *PtrVND6-C1^{IR}* in xylem (X), phloem (P), young shoots (S), and leaves (L). The error bars represent SEs from three biological replicates. (*D*) Gene and protein structures of *PtrVND6-C1* and *PtrVND6-C1^{IR}*. (*i*) Genomic DNA of *PtrVND6-C1* with three exons (E1–3) and two introns (I1–2). (*ii*) *PtrVND6-C1* mRNA has three exons (E1–3). (*iii*) *PtrVND6-C1^{IR}* mRNA has three exons (E1–3) and a retained intron (I2) that contains a PTC. We also manually aligned the I2 of each of the PtrVND6 genes and found no branch point-specific sequences for IR genes. (*iv*) PtrVND6-C1 is composed of a conserved N-terminal NAC domain containing β′, α1a/b, β1–6 subdomains, and a C-terminal activation domain. (*v*) PtrVND6-C1^{IR} has an incomplete N-terminal NAC domain consisting of β′, α1a/b, β1–5 subdomains, and 28 aa translated from the front part of intron 3 (before PTC). (*E*) Western blot analysis using recombinant PtrVND6-C1^{IR} and SDX nuclear proteins with the PtrVND6-C1 NAC domain antibody (black stars) (*i*) or PtrVND6-C1^{IR} 28 aa-specific antibody (gray stars) (*ii*). (*F*) SDX protoplast transactivation assays overexpressing GFP (control) or PtrVND6-A1, -A2, -B1, -B2, -C1, -C2, or -C1^{IR}. The transcript abundance of PtrMYB021 was detected using qRT-PCR. The error bars represent SEs from three biological replicates. Statistical significance was estimated using the Student *t* test (**$P < 0.05$; compared with control). (*G*) EMSA using PtrVND6-C1 or PtrVND6-C1^{IR} recombinant proteins with *PtrMYB021* promoter fragments labeled by biotin. *PtrMYB021* promoter fragments without biotin labeling were used as competitors. The arrow shows the shifted band representing the protein–DNA complex.

expression of *PtrMYB021* by a mechanism that is not mediated by direct protein–DNA interaction.

PtrVND6-C1^{IR} has characteristics of dominant negatives, because PtrVND6-C1^{IR} suppresses its downstream genes (*PtrMYB021*), lacks an activation domain, lacks DNA binding ability, but retains the protein dimerization domain (6, 21, 23). Dominant negatives are also known to act as posttranslational regulators by forming protein heterodimers with their targets through protein dimerization domains, thereby suppressing the function of the targets (6, 23). NAC TFs contain a highly conserved protein dimerization domain (26). Therefore, we tested whether PtrVND6-C1^{IR} can form heterodimers with each of the six full-size PtrVNDs to suppress their

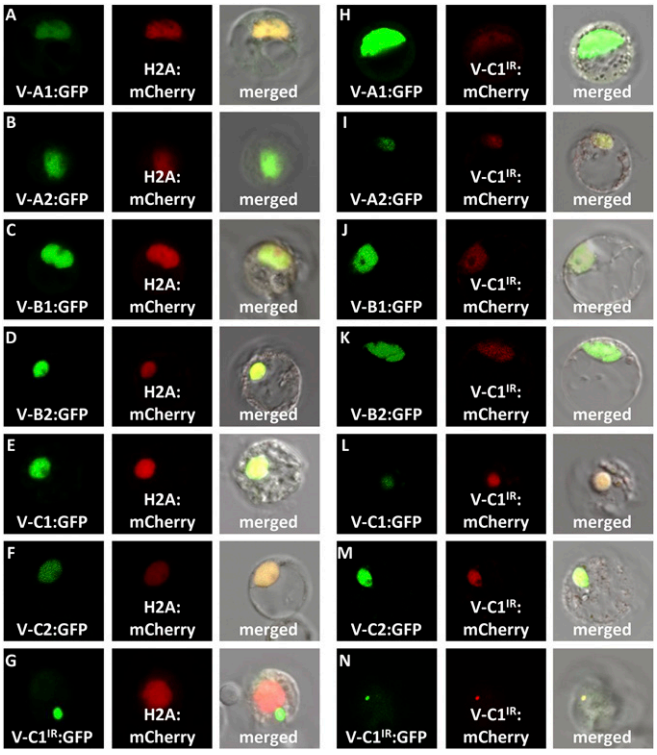

Fig. 2. Subcellular colocalization demonstrates that PtrVND6-C1^{IR} can be translocated from cytoplasmic foci into the nucleus. (*A*) PtrVND6-A1:GFP, (*B*) PtrVND6-A2:GFP, (*C*) PtrVND6-B1:GFP, (*D*) PtrVND6-B2:GFP, (*E*) PtrVND6-C1:GFP, and (*F*) PtrVND6-C2:GFP localized with H2A:mCherry in the nucleus, but (*G*) PtrVND6-C1^{IR}:GFP localized in cytoplasmic foci. PtrVND6-C1^{IR}:mCherry can be translocated into the nucleus by (*H*) PtrVND6-A1:GFP, (*I*) PtrVND6-A2:GFP, (*J*) PtrVND6-B1:GFP, (*K*) PtrVND6-B2:GFP, (*L*) PtrVND6-C1:GFP, and (*M*) PtrVND6-C2:GFP. (*N*) PtrVND6-C1^{IR}:GFP and PtrVND6-C1^{IR}:mCherry colocalized in cytoplasmic foci. The diameter of the SDX protoplasts is ~30 μm.

functions. To test for the formation of these heterodimers, we first determined the subcellular locations of PtrVND6-C1^{IR} and the six full-size PtrVND6s.

Each of the Six Full-Size PtrVND6s Can Translocate PtrVND6-C1^{IR} from the Cytoplasm into the Nucleus. GFP was fused to each of the six full-size PtrVND6s and PtrVND6-C1^{IR} and overexpressed in *P. trichocarpa* SDX protoplasts. *H2A*-fused mCherry was used as a nuclear marker (6). We detected both GFP and mCherry exclusively in the nucleus in ~95% of the protoplasts transfected with each of the six full-size PtrVND6s, demonstrating that all of these VNDs are exclusively colocated with H2A in the nucleus (Fig. 2 *A*–*F*). In contrast, PtrVND6-C1^{IR} is exclusively found in cytoplasmic foci in all transfected protoplasts (Fig. 2*G*). About 5% of the protoplasts showed the full-size PtrVND6s in both the nucleus and cytoplasmic foci. The sporadic location of the full-size PtrVND6s in cytoplasmic foci suggests that PtrVND6-C1^{IR} may retain these PtrVND6s in the cytoplasm through protein–protein interactions. We then tested for such interactions by determining the subcellular location of the full-size PtrVND6s in the presence of PtrVND6-C1^{IR}.

Each of the six full-size PtrVND6s fused with GFP was cotransfected with mCherry-fused PtrVND6-C1^{IR}. The full-size PtrVND6s were found in the nucleus, but PtrVND6-C1^{IR} was translocated by the full-size PtrVND6s into the nucleus (Fig. 2 *H*–*M*). We also cotransfected GFP-fused PtrVND6-C1^{IR} with mCherry-fused PtrVND6-C1^{IR} and detected both GFP and mCherry only in cytoplasmic foci (Fig. 2*N*). Therefore, PtrVND6-C1^{IR} can only be translocated into the nucleus by any of the six full-size PtrVND6s but not by itself. The translocation demonstrates that PtrVND6-C1^{IR} interacts with each of the six full-size PtrVND6s. To verify these protein–protein interactions, we then carried out BiFC in *P. trichocarpa* SDX protoplasts.

PtrVND6-C1^{IR} Dimerizes with Each of the Six Full-Size PtrVND6s in the Nucleus. To perform BiFC, CFP^{C} (amino acids 174–329) and CFP^{N} (amino acids 1–173) (6) were fused to the C terminus of PtrVND6-C1^{IR} and each of the six full-size PtrVND6s, resulting in PtrVND6-C1^{IR}:CFP^{C} and six PtrVND6s:CFP^{N}. The positive CFP signal indicates an interaction of CFP^{C} and CFP^{N} due to the heterodimerization of PtrVND6-C1^{IR} with a full-size PtrVND6. Each of the PtrVND6s:CFP^{N} was cotransfected with PtrVND6-C1^{IR}:CFP^{C} and H2A:mCherry into SDX protoplasts. The signal of CFP was colocalized with mCherry (Fig. 3 *A*, *C*, *E*, *G*, *I*, and *K*), demonstrating that PtrVND6-C1^{IR} formed a heterodimer with any of the full-size PtrVND6s and moved into the nucleus. We also cotransfected PtrVND6-C1^{IR}:CFP^{C}, PtrVND6-C1^{IR}:CFP^{N}, and H2A:mCherry and found CFP exclusively in cytoplasmic foci (Fig. 3*M*), showing that PtrVND6-C1^{IR} forms homodimers only in cytoplasmic foci. PtrVND6-C1^{IR}:CFP^{N}, PtrVND6-C1^{IR}:CFP^{C}, and each of the PtrVND6s:CFP^{N} were transfected individually as negative controls, and neither of the constructs showed a fluorescence signal (Fig. 3 *B*, *D*, *F*, *H*, *J*, *L* and *N*).

The results of BiFC and colocalization further support the characterization of PtrVND6-C1^{IR} as a dominant negative based on the formation of heterodimers with the full-size PtrVND6s to suppress their function as direct activators. Many NAC TFs are

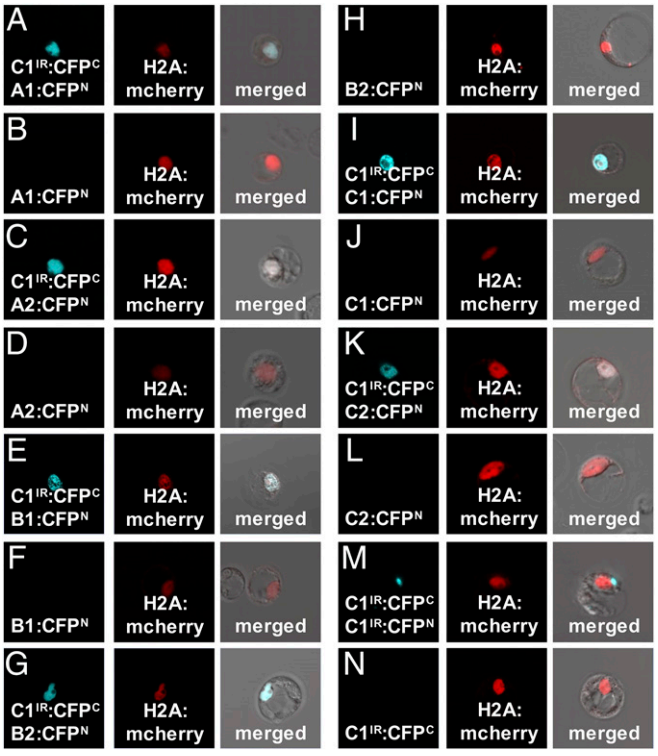

Fig. 3. BiFC of PtrVND6-C1^{IR} with each of the PtrVND6 family members. PtrVND6-C1^{IR} was fused with CFP^{C}, and each of the PtrVND6 family members was fused with CFP^{N}. CFP signal was detected in the nucleus of the SDX protoplasts transfected by H2A:mCherry and PtrVND6-C1^{IR}:CFP^{C} with (*A*) PtrVND6-A1:CFP^{N}, (*C*) PtrVND6-A2:CFP^{N}, (*E*) PtrVND6-B1:CFP^{N}, (*G*) PtrVND6-B2:CFP^{N}, (*I*) PtrVND6-C1:CFP^{N}, (*K*) PtrVND6-C2:CFP^{N}, or (*M*) PtrVND6-C1^{IR}:CFP^{N}. SDX protoplasts transfected with only (*B*) PtrVND6-A1:CFP^{N}, (*D*) PtrVND6-A2:CFP^{N}, (*F*) PtrVND6-B1:CFP^{N}, (*H*) PtrVND6-B2:CFP^{N}, (*J*) PtrVND6-C1:CFP^{N}, (*L*) PtrVND6-C2:CFP^{N}, or (*N*) PtrVND6-C1^{IR}:CFP^{C} were used as negative controls. The diameter of the SDX protoplasts is ~30 μm.

known to self-activate their own genes (6, 27); therefore, we tested whether PtrVND6-C1^{IR} can also suppress the self-activation function of the full-size PtrVND6s.

PtrVND6-C1^{IR} Suppresses the Self-Activation of the Full-Size PtrVND6s. We first tested whether the six full-size *PtrVND6*s have a self-activation function using effector–reporter-based gene transactivation assays. PtrVND6-B2, PtrVND6-C1, and PtrVND6-C2 can activate their own gene expression (Fig. S7*A*), and PtrVND6-A1, PtrVND6-A2, and PtrVND6-B1 can be activated by PtrVND6-C1 or PtrVND6-C2 (Fig. S7*B*). In the other words, *PtrVND6*s family members are either self-activated or activated by other members. Overexpression of *PtrVND6-C1^{IR}* in SDX protoplasts reduced the transcript abundance of *PtrVND6-A1*, *-A2*, *-B1*, *-B2*, and *-C2* but did not affect the expression of its full-size isoform, *PtrVND6-C1* (Fig. S8), suggesting that *PtrVND6-C1* is also controlled by other TFs, which are not affected by PtrVND6-C1^{IR}.

In our previous study, PtrSND1-A2^{IR}, the splice variant of PtrSND1-A2, also suppressed the full-size PtrSND1 functions through the formation of heterodimers (6). Of the two major NAC families, SND1 and VND6, each has an IR splice variant suppressing the transcription of their own family members. It is unknown whether there are protein–protein interactions between PtrVND6 and PtrSND1 families. We then investigated whether PtrVND6-C1^{IR} can also form heterodimers with each of the four full-size PtrSND1s (6) and whether heterodimerization occurs between PtrSND1-A2^{IR} with the six full-size PtrVND6s. To test for the formation of cross-family heterodimers, we first investigated whether PtrVND6-C1^{IR}, PtrSND1-A2^{IR}, and the six full-size PtrVND6s and the four full-size PtrSND1s are expressed in the same cell type.

***PtrVND6-C1^{IR}*, *PtrSND1-A2^{IR}*, Full-Size *PtrVND6*, and *PtrSND1* Members Are All Coexpressed in Fiber and Vessel Cells.** We used the stem cross-sections of *P. trichocarpa* (Fig. 4*A*) and our recently developed LCM to collect fibers (Fig. 4*B*), vessels (Fig. 4*C*), and a combination of three cell types (fibers + vessels + rays) (8, 9) (Fig. 4*D*). qRT-PCR demonstrated that *PtrVND6-C1^{IR}* and *PtrSND1-A2^{IR}* are expressed in fibers, vessels, and three cell types at roughly equivalent levels (Fig. 4 *E* and *F*). Similarly, all full-size *PtrVND6*s and *PtrSND1*s are expressed in fibers and vessels and three cell types (Fig. 4*G*). The presence of *PtrVND6-C1^{IR}*, *PtrSND1-A2^{IR}*, and all full-size *PtrVND6*s and *PtrSND1*s in the same cell types is essential for the proposed formation of cross-family heterodimers.

Full-Size PtrVND6s and PtrSND1s Cross-Interact with PtrVND6-C1^{IR} and PtrSND1-A2^{IR} to Translocate PtrVND6-C1^{IR} and PtrSND1-A2^{IR} from Cytoplasmic Foci into the Nucleus. To test for cross-family heterodimerization, we first tested the subcellular localization of PtrVND6-C1^{IR} with each of the four full-size PtrSND1s and PtrSND1-A2^{IR} with each of the six full-size PtrVND6s. PtrVND6-C1^{IR} was translocated from the cytosol (Fig. 2*G*) into the nucleus by any of the four full-size PtrSND1s (Fig. 5 *A*–*D*). Similarly, PtrSND1-A2^{IR} was translocated from the cytosol (6) into the nucleus by each of the six full-size PtrVND6s (Fig. 5 *E*–*J*). The translocation of the splice variants can only be achieved by the full-size members, because PtrVND6-C1^{IR} cannot translocate PtrSND1-A2^{IR} into the nucleus and vice versa (Fig. 5 *K* and *L*).

PtrVND6-C1^{IR} and PtrSND1-A2^{IR} Form Cross-Family Heterodimers with PtrSND1s and PtrVND6s. BiFC was used to test for protein–protein interactions between PtrVND6-C1^{IR} and each of the four full-size PtrSND1s and between PtrSND1-A2^{IR} and each of the six full-size PtrVND6s. We cotransfected PtrVND6-C1^{IR}:CFP^{C} with each of the four PtrSND1s:CFP^{N} and also cotransfected PtrSND1-A2^{IR}:CFP^{C} with each of the six PtrVND6s:CFP^{N} into

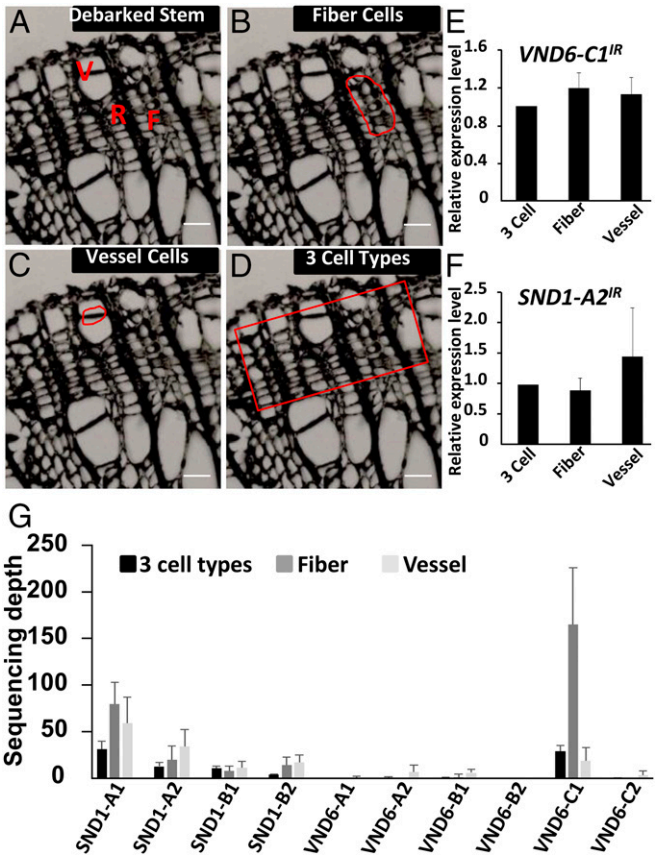

Fig. 4. Fiber, vessel, and three cell types collected by LCM and the transcript abundance of the *PtrVND6* and *PtrSND1* families in these cell types. (*A*) Cross-section of the debarked stem from the 17th internode of *P. trichocarpa*. F, fiber cells; R, ray cells; V, vessel cells. LCM was used to collect (*B*) fiber cells, (*C*) vessel cells, and (*D*) three cell types. (Scale bars, 25 μm.) qRT-PCR was used to detect the transcript abundance of (*E*) PtrVND6-C1^{IR} and (*F*) PtrSND1-A2^{IR} in different cell types. (*G*) RNA-seq analysis was used to estimate the transcript abundance of full-length *PtrVND6* and *PtrSND1*. The error bars represent SE from three biological replicates.

SDX protoplasts. The CFP signal in all transfected protoplasts was colocalized with mCherry in the nucleus (Fig. 6 *A*, *C*, *E*, *G*, *I*, *K*, *M*, *O*, *Q*, and *S*), demonstrating cross-family heterodimerization. As negative controls, we transfected PtrVND6-C1^{IR}:CFP^{C}, PtrSND1-A2^{IR}:CFP^{C}, and each of the full-size PtrSND1s-CFP^{N} and PtrVND6s-CFP^{N} individually. CFP signal was not detected (Fig. 6 *B*, *D*, *F*, *H*, *J*, *L*, *N*, *P*, *R*, and *T*). We then tested whether cross-family heterodimerization suppresses the self-activation functions of full-size PtrSND1s and PtrVND6s.

PtrVND6-C1^{IR} and PtrSND1-A2^{IR} Inhibit the Self-Activation of Full-Size PtrVND6s and PtrSND1s. We overexpressed *PtrVND6-C1^{IR}* in SDX protoplasts and found that the transcript abundance of each of the four full-size *PtrSND1*s was reduced (Fig. 7*A*), demonstrating that the function of each of the four full-size PtrSND1s was suppressed by PtrVND6-C1^{IR} (Fig. 8). Similarly, overexpression of PtrSND1-A2^{IR} reduced the transcript abundance of each of the six full-size *PtrVND6*s (Fig. 7*B*). The results demonstrate a plausible mechanism where cross-family heterodimerization may suppress PtrVND6 and PtrSND1 self-activation (Fig. 8).

These results combined with the previous study of PtrSND1-A2^{IR} regulating the PtrSND1 family (6) demonstrate that PtrVND6 and PtrSND1 families can cross-regulate each other through their alternative splice variants (Fig. 8). The formation of these heterodimers suggests a general cross-regulation mechanism

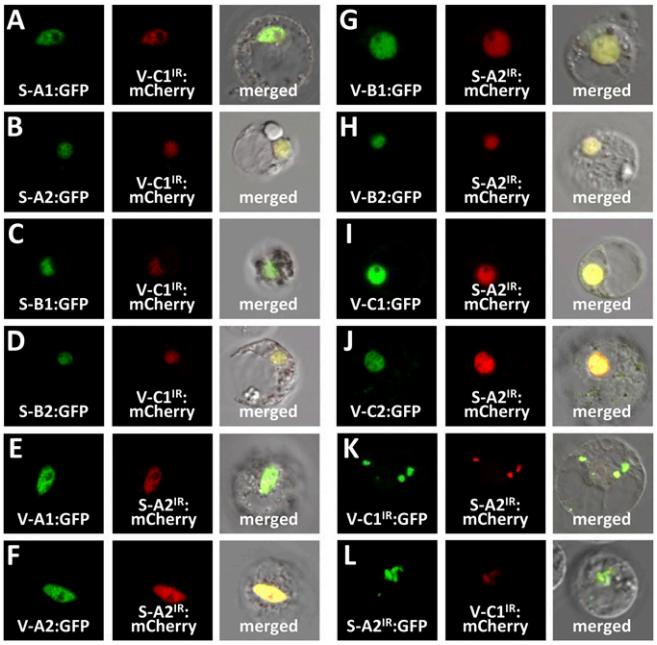

Fig. 5. Subcellular colocalization of PtrVND6-C1^{IR} with each of the PtrSND1 family members and PtrSND1-A2^{IR} with each of the PtrVND6 family members in SDX protoplasts. PtrVND6-C1^{IR} and PtrSND1-A2^{IR} were fused to either GFP or mCherry, and full-length PtrVND6 and PtrSND1 members were fused to GFP. PtrVND6-C1^{IR}:mCherry colocalized with (*A*) PtrSND1-A1:GFP, (*B*) PtrSND1-A2:GFP, (*C*) PtrSND1-B1:GFP, or (*D*) PtrSND1-B2:GFP in the nucleus. PtrSND1-A2^{IR}:mCherry colocalized with (*E*) PtrVND6-C1:GFP, (*F*) PtrVND6-A2:GFP, (*G*) PtrVND6-B1:GFP, (*H*) PtrVND6-B2:GFP, (*I*) PtrVND6-C1:GFP, or (*J*) PtrVND6-C2:GFP in the nucleus. (*K*) PtrVND6-C1^{IR}:GFP colocalized with PtrSND1-A2^{IR}:mCherry in the cytoplasmic foci. (*L*) PtrSND1-A2^{IR}:GFP colocalized with PtrVND6-C1^{IR}:mCherry in the cytoplasmic foci. The diameter of the SDX protoplasts is ~30 μm.

to maintain the homeostasis of the expression of PtrVND6 and PtrSND1 family members through their splice variants, PtrVND6-C1^{IR} and PtrSND1-A2^{IR}, providing xylem-specific NAC TF regulation in fibers and vessels in wood formation.

Discussion

VND6 and *SND1* are distinct gene families based on their protein sequences in many plant species, including *P. trichocarpa* (6), *Arabidopsis* (10, 11), rice (28), maize (29), banana (30), and loquat (31). These two families act as transactivators with distinct functions in the regulation of SCW differentiation (3, 10–12). VND6 regulates the differentiation of vessels (3, 10, 12), while SND1 induces SCW thickening in fibers (11). Overexpression of *VND6* and *SND1* in *Arabidopsis* leads to abnormal xylem development or retarded growth (5, 10, 11). Regulation of *VND6* and *SND1* is necessary for normal growth and development (6). In *P. trichocarpa*, *VND6* and *SND1* (6) each has an IR splice variant. The existence of these unique regulatory variants in *P. trichocarpa* suggests a higher level of functional differentiation in xylogenesis or additional regulation to maintain homeostasis.

In both animals and plants, alternative splicing events regulate homeostasis in different states of development, differentiation, and metabolism (32, 33). More than 60% of intron-containing genes in plants have transcript variants derived from alternative splicing (34, 35). A major mode of alternative splicing is the retention of introns (36), which often results in a truncated protein due to premature termination (19, 23, 37, 38). If such truncated proteins are derived from TF genes, they may act as dominant negatives to suppress the function of the cognate TFs (6, 34, 35, 38). In *P. trichocarpa*, we previously identified a dominant negative, *PtrSND1-A2^{IR}*, derived from the IR variant of *PtrSND1-A2*, which suppresses the self-activation of three out of the four *PtrSND1* members (except *PtrSND1-A2*) and their protein functions (6). PtrSND1-A2^{IR} was the first discovered dominant negative that suppresses multiple members within its own family (6). Here we demonstrated that PtrVND6-C1^{IR}, another dominant negative derived from an IR variant of *PtrVND6-C1*, can also suppress multiple targets within its own family (Fig. S8). PtrVND6-C1^{IR} and PtrSND1-A2^{IR} both exert within-family regulation.

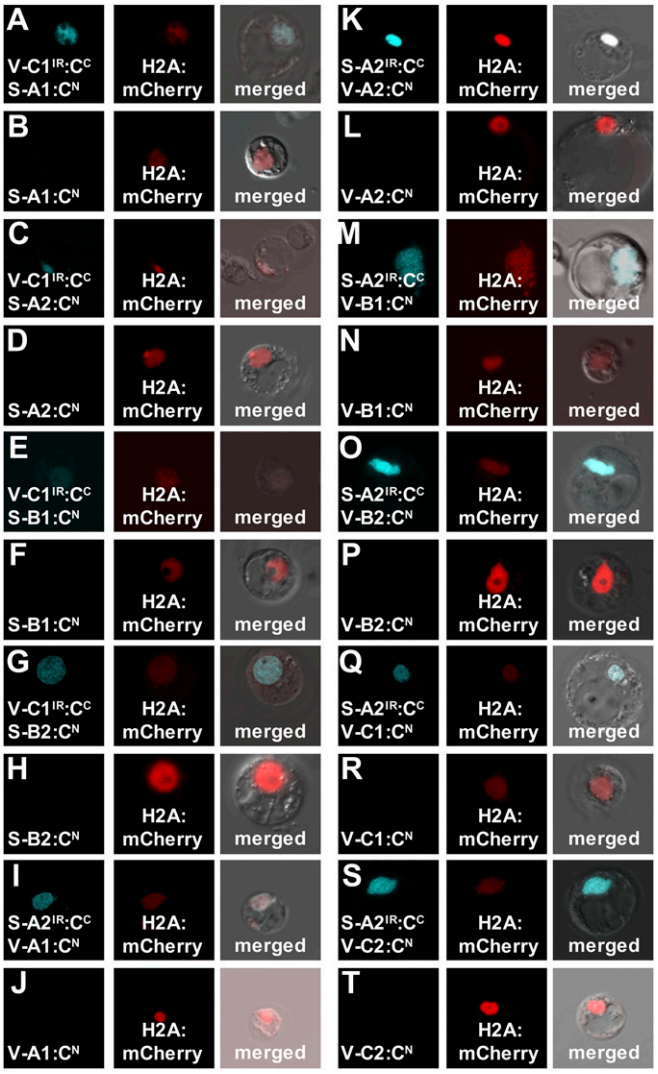

Fig. 6. BiFC of PtrVND6-C1^{IR} with each of the PtrSND1 family members and PtrSND1-A2^{IR} with each of the PtrVND6 family members in SDX protoplasts. PtrVND6-C1^{IR} and PtrSND1-A2^{IR} were fused with CFP^{C}, and full-length PtrVND6 and PtrSND1 members were fused to CFP^{N}. H2A was fused with mCherry as a nuclear marker. CFP signal was detected in the nucleus of the SDX protoplasts transfected by H2A:mCherry with the following combinations: (*A*) PtrSND1-A1:CFP^{N}, (*C*) PtrSND1-A2:CFP^{N}, (*E*) PtrSND1-B1:CFP^{N}, or (*G*) PtrSND1-B2:CFP^{N} each with PtrVND6-C1^{IR}:CFP^{C}; (*I*) PtrVND6-A1:CFP^{N}, (*K*) PtrVND6-A2:CFP^{N}, (*M*) PtrVND6-B1:CFP^{N}, (*O*) PtrVND6-B2:CFP^{N}, (*Q*) PtrVND6-C1:CFP^{N}, or (*S*) PtrVND6-C2:CFP^{N} each with PtrSND1-A2^{IR}:CFP^{C}. No CFP signal was detected from SDX transfected with only (*B*) PtrSND1-A1:CFP^{N}, (*D*) PtrSND1-A2:CFP^{N}, (*F*) PtrSND1-B1:CFP^{N}, (*H*) PtrSND1-B2:CFP^{N}, (*J*) PtrVND6-A1:CFP^{N}, (*L*) PtrVND6-A2:CFP^{N}, (*N*) PtrVND6-B1:CFP^{N}, (*P*) PtrVND6-B2:CFP^{N}, (*R*) PtrVND6-C1:CFP^{N}, or (*T*) PtrVND6-C2:CFP^{N}. The diameter of the SDX protoplasts is ~30 μm.

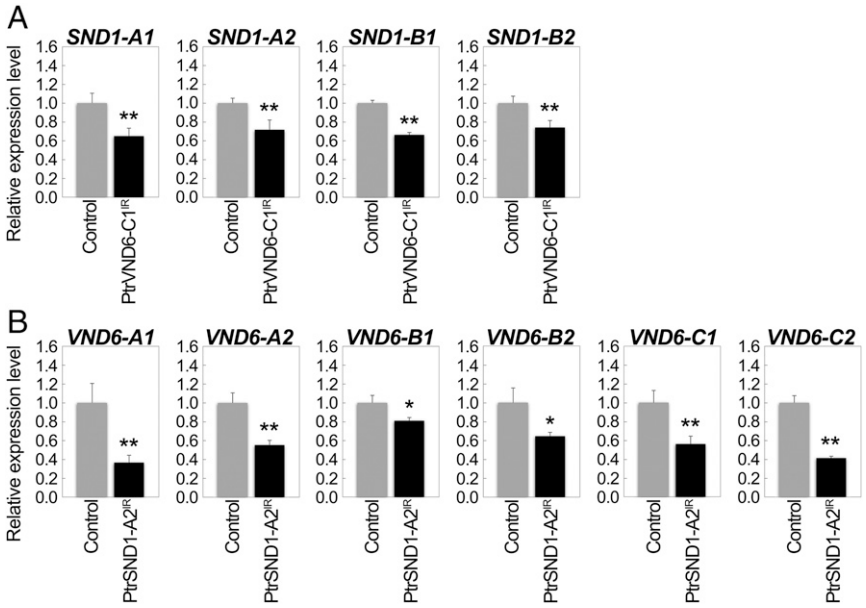

Fig. 7. Cross-regulation between *PtrVND6* and *PtrSND1* families through PtrVND6-C1^{IR} and PtrSND1-A2^{IR}. qRT-PCR was used to detect the transcript abundance of (*A*) *PtrSND1-A1*, *-A2*, *- B1*, or *-B2* in SDX protoplasts overexpressing *GFP* (control) or *PtrVND6-C1^{IR}* and (*B*) *PtrVND6-A1*, *-A2*, *-B1*, *-B2*, *-C1*, or *-C2* in SDX protoplasts overexpressing *GFP* or *PtrSND1-A2^{IR}*. The control values in *A* and *B* were set as 1, and the error bars represent SEs from two to three biological replicates. Statistical significance was estimated using the Student *t* test (**P* < 0.1; ***P* < 0.05).

We now also found that PtrVND6-C1^{IR} and PtrSND1-A2^{IR} can exert cross-family (reciprocal) regulation. PtrVND6-C1^{IR} suppresses all *PtrSND1* members, while PtrSND1-A2^{IR} suppresses all *PtrVND6* members. The reciprocal regulation of the PtrVND6 and PtrSND1 families (Figs. 7 and 8) depends on the formation of heterodimers between IR variants and their full-size members. Cytoplasmic foci are the locations of the free IR variants (Fig. 5 *K* and *L*). In the presence of the full-size members, the IR variants form heterodimers in the cytosol and are subsequently translocated into the nucleus (Figs. 5 and 6). To carry out the reciprocal family regulation, both families have to be expressed in the same cells. Our LCM results showed that PtrVND6-C1^{IR}, PtrSND1-A2^{IR}, and their full-size family members are all expressed in both fibers and vessels (Fig. 4 *E* and *F*).

In our previous work, we showed that the PtrSND1-A2IR was able to suppress the expression of the PtrSND1 family except PtrSND1-A2, its cognate TF (6), raising the question of what regulates PtrSND1-A2 to maintain the down-regulation of this family. We have now identified PtrVND6-C1^{IR} as this unknown regulator that can suppress *PtrSND1-A2* expression. Similarly, PtrVND6-C1^{IR} can suppress all members of the *PtrVND6* family except *PtrVND6-C1*, and *PtrVND6-C1* can be suppressed by PtrSND1-A2^{IR}. This cross-family reciprocal regulation by these two splice variants provides a mechanism to maintain the homeostasis of the expression of both PtrVND6 and PtrSND1 families. This unique mechanism has not been reported for TF trans-regulation of distinct families with related functions, in this case wood formation. In *Arabidopsis*, the mRNA of VND6 and SND1 families do not have splice variants (10, 11), suggesting a relatively simple regulation of SCW differentiation in herbaceous plants. In contrast, perennial woody plants develop woody stems and undergo secondary growth, which requires more complex regulation. The discovery of PtrVND6-C1^{IR}– and PtrSND1-A2^{IR}–based reciprocal cross-regulation implicates a higher level of transcriptional control in perennial woody plants during wood formation.

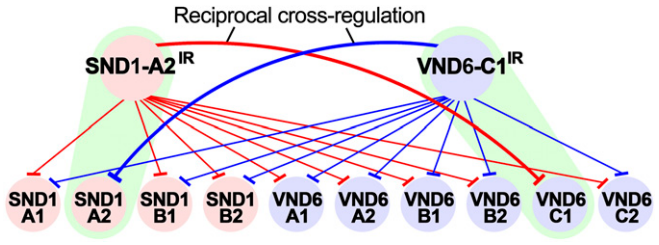

Fig. 8. Cross-regulation between the *PtrVND6* and *PtrSND1* families through PtrVND6-C1^{IR} and PtrSND1-A2^{IR}. PtrSND1-A2^{IR} suppresses the transcript abundance of the *PtrSND1* and *PtrVND6* families (red edges) except *PtrSND1-A2* (green highlight). PtrVND6-C1^{IR} suppresses *PtrSND1* and *PtrVND6* families (blue edges) except *PtrVND6-C1* (green highlight).

The dimerization domain of a NAC TF is located in the highly conserved N-terminal NAC domain (26). The NAC domain protein sequence identities within the PtrVND6 and PtrSND1 family are at least 81% and 87%, respectively, and are at least 75% between PtrVND6 and PtrSND1 families (6). In our LCM results, 72 NAC TFs are expressed in both fibers and vessels. Due to the highly conserved NAC domain within the NAC family, splice variants may exert a broader interfamily regulation through the formation of heterodimers with these 72 NAC domain proteins. Members of many other TF families, such as MADS-box, bZIP, MYB, WRKY, and bHLH, form functional dimers (39, 40). If the mRNAs of these TFs have splice variants leading to truncated proteins with protein dimerization domains, then these splice variants may also act as dominant negatives to regulate their family members. These results suggest that reciprocal homeostatic mechanisms exist for other TF families, where splice variants may provide higher level transcriptional regulation of complex processes in adaptation, differentiation, development, and growth.

Materials and Methods

Plant materials, RNA extraction, qRT-PCR, PCR cloning, RNA-seq, Western blotting, SDX nuclear protein preparation, EMSA, effector–reporter-based gene transactivation assays, protoplast transfection, protein subcellular localization, and BiFC are described in detail in *SI Materials and Methods*. Primer sequences are listed in Table S1.

ACKNOWLEDGMENTS. We thank the National Natural Science Foundation of China (NSFC) for financial support from Grants 31430093, 31522014, 31370593, and 31670674. This work was also supported by US Office of Science (Biological and Environmental Research), Department of Energy Grant DE-SC000691 and the North Carolina State University Jordan Family Distinguished Professor Endowment.

1. Sarkanen KV (1976) Renewable resources for the production of fuels and chemicals. *Science* 191:773–776.
2. Chiang VL (2002) From rags to riches. *Nat Biotechnol* 20:557–558.
3. Ohtani M, et al. (2011) A NAC domain protein family contributing to the regulation of wood formation in poplar. *Plant J* 67:499–512.
4. Lin YC, et al. (2013) SND1 transcription factor-directed quantitative functional hierarchical genetic regulatory network in wood formation in Populus trichocarpa. *Plant Cell* 25:4324–4341.
5. Nakano Y, Yamaguchi M, Endo H, Rejab NA, Ohtani M (2015) NAC-MYB-based transcriptional regulation of secondary cell wall biosynthesis in land plants. *Front Plant Sci* 6:288.
6. Li Q, et al. (2012) Splice variant of the SND1 transcription factor is a dominant negative of SND1 members and their regulation in *Populus trichocarpa*. *Proc Natl Acad Sci USA* 109:14699–14704.
7. Zhao Y, Sun J, Xu P, Zhang R, Li L (2014) Intron-mediated alternative splicing of WOOD-ASSOCIATED NAC TRANSCRIPTION FACTOR1B regulates cell wall thickening during fiber development in *Populus* species. *Plant Physiol* 164:765–776.
8. Wang JP, et al. (2015) Phosphorylation is an on/off switch for 5-hydroxyconiferaldehyde O-methyltransferase activity in poplar monolignol biosynthesis. *Proc Natl Acad Sci USA* 112:8481–8486.
9. Chen HC, et al. (2014) Systems biology of lignin biosynthesis in *Populus trichocarpa*: Heteromeric 4-coumaric acid:coenzyme A ligase protein complex formation, regulation, and numerical modeling. *Plant Cell* 26:876–893.
10. Kubo M, et al. (2005) Transcription switches for protoxylem and metaxylem vessel formation. *Genes Dev* 19:1855–1860.
11. Zhong R, Demura T, Ye ZH (2006) SND1, a NAC domain transcription factor, is a key regulator of secondary wall synthesis in fibers of *Arabidopsis*. *Plant Cell* 18: 3158–3170.
12. Ko JH, Yang SH, Park AH, Lerouxel O, Han KH (2007) ANAC012, a member of the plant-specific NAC transcription factor family, negatively regulates xylary fiber development in *Arabidopsis thaliana*. *Plant J* 50:1035–1048.
13. Yamaguchi M, et al. (2010) VASCULAR-RELATED NAC-DOMAIN6 and VASCULAR-RELATED NAC-DOMAIN7 effectively induce transdifferentiation into xylem vessel elements under control of an induction system. *Plant Physiol* 153:906–914.
14. Yamaguchi M, et al. (2011) VASCULAR-RELATED NAC-DOMAIN7 directly regulates the expression of a broad range of genes for xylem vessel formation. *Plant J* 66:579–590.
15. Kim WC, et al. (2013) MYB46 directly regulates the gene expression of secondary wall-associated cellulose synthases in *Arabidopsis*. *Plant J* 73:26–36.
16. Kim WC, Kim JY, Ko JH, Kang H, Han KH (2014) Identification of direct targets of transcription factor MYB46 provides insights into the transcriptional regulation of secondary wall biosynthesis. *Plant Mol Biol* 85:589–599.
17. Ohashi-Ito K, Oda Y, Fukuda H (2010) Arabidopsis VASCULAR-RELATED NAC-DOMAIN6 directly regulates the genes that govern programmed cell death and secondary wall formation during xylem differentiation. *Plant Cell* 22:3461–3473.
18. Gaston K, Jayaraman P-S (2003) Transcriptional repression in eukaryotes: Repressors and repression mechanisms. *Cell Mol Life Sci* 60:721–741.
19. Seo PJ, Hong SY, Kim SG, Park CM (2011b) Competitive inhibition of transcription factors by small interfering peptides. *Trends Plant Sci* 16:541–549.
20. Amoutzias GD, Robertson DL, Van de Peer Y, Oliver SG (2008) Choose your partners: Dimerization in eukaryotic transcription factors. *Trends Biochem Sci* 33:220–229.
21. Staudt AC, Wenkel S (2011) Regulation of protein function by 'microProteins'. *EMBO Rep* 12:35–42.
22. Eguen T, Straub D, Graeff M, Wenkel S (2015) MicroProteins: Small size-big impact. *Trends Plant Sci* 20:477–482.
23. Seo PJ, Kim MJ, Ryu JY, Jeong EY, Park CM (2011a) Two splice variants of the IDD14 transcription factor competitively form nonfunctional heterodimers which may regulate starch metabolism. *Nat Commun* 2:303.
24. Seo PJ, et al. (2012) A self-regulatory circuit of CIRCADIAN CLOCK-ASSOCIATED1 underlies the circadian clock regulation of temperature responses in Arabidopsis. *Plant Cell* 24: 2427–2442.
25. Lin YC, et al. (2014) A simple improved-throughput xylem protoplast system for studying wood formation. *Nat Protoc* 9:2194–2205.
26. Ernst HA, Olsen AN, Larsen S, Lo Leggio L (2004) Structure of the conserved domain of ANAC, a member of the NAC family of transcription factors. *EMBO Rep* 5:297–303.
27. Wang H, Zhao Q, Chen F, Wang M, Dixon RA (2011) NAC domain function and transcriptional control of a secondary cell wall master switch. *Plant J* 68:1104–1114.
28. Ambavaram MMR, Krishnan A, Trijatmiko KR, Pereira A (2011) Coordinated activation of cellulose and repression of lignin biosynthesis pathways in rice. *Plant Physiol* 155: 916–931.
29. Peng X, et al. (2015) Genomewide identification, classification and analysis of NAC type gene family in maize. *J Genet* 94:377–390.
30. Negi S, Tak H, Ganapathi TR (2015) In vitro xylem vessel elements formation from banana embryogenic cells and expression analysis of vessel development-related genes. *Plant Biotechnol Rep* 9:47–54.
31. Xu Q, et al. (2015) A NAC transcription factor, EjNAC1, affects lignification of loquat fruit by regulating lignin. *Postharvest Biol Technol* 102:25–31.
32. Yabas M, Elliott H, Hoyne GF (2015) The role of alternative splicing in the control of immune homeostasis and cellular differentiation. *Int J Mol Sci* 17:E3.
33. Bazin J, Bailey-Serres J (2015) Emerging roles of long non-coding RNA in root developmental plasticity and regulation of phosphate homeostasis. *Front Plant Sci* 6: 400.
34. Syed NH, Kalyna M, Marquez Y, Barta A, Brown JW (2012) Alternative splicing in plants—Coming of age. *Trends Plant Sci* 17:616–623.
35. Filichkin S, Priest HD, Megraw M, Mockler TC (2015) Alternative splicing in plants: Directing traffic at the crossroads of adaptation and environmental stress. *Curr Opin Plant Biol* 24:125–135.
36. Ner-Gaon H, et al. (2004) Intron retention is a major phenomenon in alternative splicing in *Arabidopsis*. *Plant J* 39:877–885.
37. Seo PJ, Park MJ, Park CM (2013) Alternative splicing of transcription factors in plant responses to low temperature stress: Mechanisms and functions. *Planta* 237: 1415–1424.
38. Kelemen O, et al. (2013) Function of alternative splicing. *Gene* 514:1–30.
39. Eulgem T, Rushton PJ, Robatzek S, Somssich IE (2000) The WRKY superfamily of plant transcription factors. *Trends Plant Sci* 5:199–206.
40. Ledent V, Vervoort M (2001) The basic helix-loop-helix protein family: Comparative genomics and phylogenetic analysis. *Genome Res* 11:754–770.
41. Shi R, et al. (2017) Tissue and cell-type co-expression networks of transcription factors and wood component genes in *Populus trichocarpa*. *Planta* 245:927–938.
42. Trapnell C, Pachter L, Salzberg SL (2009) TopHat: Discovering splice junctions with RNA-seq. *Bioinformatics* 25:1105–1111.
43. Robinson MD, Oshlack A (2010) A scaling normalization method for differential expression analysis of RNA-seq data. *Genome Biol* 11:R25.
44. Jin J, Zhang H, Kong L, Gao G, Luo J (2014) PlantTFDB 3.0: A portal for the functional and evolutionary study of plant transcription factors. *Nucleic Acids Res* 42: D1182–D1187.
45. Illumine (2010) *TruSeq RNA Sample Preparation Guide*. Available at https://support.illumina.com/downloads/truseq_rna_sample_preparation_guide_15008136.html. Accessed October 13, 2017.
46. Tuskan GA, et al. (2006) The genome of black cottonwood, *Populus trichocarpa* (Torr. & Gray). *Science* 313:1596–1604.
47. Li H, et al.; 1000 Genome Project Data Processing Subgroup (2009) The sequence alignment/map format and SAMtools. *Bioinformatics* 25:2078–2079.
48. Thorvaldsdóttir H, Robinson JT, Mesirov JP (2013) Integrative genomics viewer (IGV): High-performance genomics data visualization and exploration. *Brief Bioinform* 14: 178–192.
49. Li W, et al. (2014) A robust chromatin immunoprecipitation protocol for studying transcription factor-DNA interactions and histone modifications in wood-forming tissue. *Nat Protoc* 9:2180–2193.
50. Zhong R, Lee C, Ye ZH (2010) Global analysis of direct targets of secondary wall NAC master switches in Arabidopsis. *Mol Plant* 3:1087–1103.
51. Yoo SD, Cho YH, Sheen J (2007) Arabidopsis mesophyll protoplasts: A versatile cell system for transient gene expression analysis. *Nat Protoc* 2:1565–1572.
52. Waadt R, et al. (2008) Multicolor bimolecular fluorescence complementation reveals simultaneous formation of alternative CBL/CIPK complexes in planta. *Plant J* 56:505–516.